THE QUARTER-POINT QUADRATIC ISOPARAMETRIC ELEMENT AS A SINGULAR ELEMENT FOR CRACK PROBLEMS

M.A. Hussain, W.E. Lorensen and G. Pflegl
Department of the Army
Watervliet Arsenal
Watervliet, New York 12189

SUMMARY

The quadratic isoparametric elements which embody the inverse square root singularity are used for calculating the stress intensity factors at tips of cracks. The strain singularity at a point or an edge is obtained in a simple manner by placing the mid-side nodes at quarter points in the vicinity of the crack tip or an edge. These elements are implemented in NASTRAN as dummy elements. The method eliminates the use of special crack tip elements and in addition, these elements satisfy the constant strain and rigid body modes required for convergence.

INTRODUCTION

In "Crack Tip Finite Elements are Unnecessary", Henshell and Shaw (ref. 1) reported that the inverse of the Jacobian associated with the coordinate transformation becomes singular at a point when the mid-side nodes for two-dimensional eight-point quadrilateral elements are placed at quarter points. Interestingly enough, the same singularity was discovered independently by Barsoum (ref. 2) for two-dimensional, as well as, three-dimensional quadratic isoparametric elements. It was then natural to investigate the order of the singularity and it was found that the singularity was precisely of the order one-half for the strains, a phenomenon encountered in linear fracture mechanics. This remarkable phenomenon completely eliminates the necessity of incorporating special crack-tip elements (ref. 3, 4 and 5) and has additional advantages over the special crack-tip elements, namely; it satisfies constant strain and rigid body modes. The special crack-tip elements were introduced in the literature to avoid the extremely fine grid mesh required in the vicinity of the crack and the cumbersome extrapolation needed when using regular finite elements (ref. 6 and 7).

Advanced versions of NASTRAN (ref. 8), as well as some general purpose programs have such isoparametric elements. Hence, by judicious choice of nodes, accurate crack-tip elements can be formulated and stress intensity factors for cracks and flaws can be computed.

In this paper, after a brief review of the two and three-dimensional formulation, we discuss the implementation of the two-dimensional quadrilateral and three-dimensional brick elements as NASTRAN dummy user elements.

Lastly, test problems are done to assess the accuracy. Stress intensity factors are computed for a C-shaped specimen. The C-shaped fracture toughness method has been accepted by ASTM as a standard test for thick-walled cylinders.

SYMBOLS

(x,y)	Cartesian coordinates
(ξ,η)	Curvilinear coordinates
x_i,y_i,ξ_i,η_i	Grid point coordinates
N_i	Shape function at grid point i
u,v	Cartesian displacements
$\{\varepsilon\}$	Strain vector
$[J]$	Jacobian matrix
$\{\sigma\}$	Stress vector
$[D]$	Stress-strain matrix
$[K]$	Element stiffness matrix
E,G,ν	Elastic constants
K_I,K_{II}	Stress intensity factors
r,θ	Local cylindrical coordinates
$\{F\}^e$	Equivalent nodal forces

THE TWO-DIMENSIONAL CASE

Following the notation of Zienkiewicz (ref. 9) the eight node element in Cartesian coordinates (x,y) is formulated by mapping its geometry into the curvilinear space (ξ,η) of the normalized square $(-1 \leq \xi \leq 1, -1 \leq \eta \leq 1)$ by quadratic shape functions of the 'Serendipity' family (ref. 9):

$$x = \sum_{i=1}^{8} N_i(\xi,\eta)x_i \ ,$$

$$y = \sum_{i=1}^{8} N_i(\xi,\eta)y_i \ ,$$

$$N_i = [(1+\xi\xi_i)(1+\eta\eta_i) - (1-\xi^2)(1+\eta\eta_i) - (1-\eta^2)(1+\xi\xi_i)]\ \xi_i^2\ \eta_i^2/4$$
$$+ (1-\xi^2)(1+\eta\eta_i)(1-\xi_i^2)\eta_i^2/2 + (1-\eta^2)(1+\xi\xi_i)(1-\eta_i^2)\ \xi_i^2/2 \ , \qquad (1)$$

where N_i is the shape function at node i whose Cartesian and curvilinear coordinates are (x_i,y_i) and (ξ_i,η_i) respectively. The details of the shape functions and the numbering sequence are given in figure 1. The same shape functions are used to interpolate the displacements within the element, hence the name isoparametric:

$$u = \sum_{i=1}^{8} N_i(\xi,\eta)u_i \ ,$$

$$v = \sum_{i=1}^{8} N_i(\xi,\eta)v_i \ . \qquad (2)$$

The stiffness matrix is found in the usual way as follows:

$$\{\varepsilon\} = \begin{Bmatrix} \varepsilon_x \\ \varepsilon_y \\ \gamma_{xy} \end{Bmatrix} = \begin{bmatrix} \frac{\partial}{\partial x} & 0 \\ 0 & \frac{\partial}{\partial y} \\ \frac{\partial}{\partial x} & \frac{\partial}{\partial y} \end{bmatrix} \begin{Bmatrix} u \\ v \end{Bmatrix} . \qquad (3)$$

Substituting from equation (2) into equation (3) we have:

$$\{\varepsilon\} = [B] \begin{Bmatrix} \vdots \\ u_i \\ v_i \\ \vdots \end{Bmatrix} = [\ldots\ B_i\ \ldots] \begin{Bmatrix} \vdots \\ u_i \\ v_i \\ \vdots \end{Bmatrix} , \qquad (4)$$

where

$$[B_i] = \begin{bmatrix} \frac{\partial N_i}{\partial x} & 0 \\ 0 & \frac{\partial N_i}{\partial y} \\ \frac{\partial N_i}{\partial x} & \frac{\partial N_i}{\partial y} \end{bmatrix} . \qquad (5)$$

By the rules of partial differentiation we obtain

$$\begin{Bmatrix} \frac{\partial N_i}{\partial x} \\ \frac{\partial N_i}{\partial y} \end{Bmatrix} = [J]^{-1} \begin{Bmatrix} \frac{\partial N_i}{\partial \xi} \\ \frac{\partial N_i}{\partial \eta} \end{Bmatrix} \tag{6}$$

where [J], the Jacobian matrix, by virtue of equation (1) is given by

$$[J] = \begin{bmatrix} \frac{\partial x}{\partial \xi} & \frac{\partial y}{\partial \xi} \\ \frac{\partial x}{\partial \eta} & \frac{\partial y}{\partial \eta} \end{bmatrix} = \begin{bmatrix} - - - & \frac{\partial N_i}{\partial \xi} & - - - \\ - - - & \frac{\partial N_i}{\partial \eta} & - - - \end{bmatrix} \begin{bmatrix} | & | \\ | & | \\ x_i & y_i \\ | & | \\ | & | \end{bmatrix} . \tag{7}$$

The stress components are given by

$$\{\sigma\} = \begin{Bmatrix} \sigma_x \\ \sigma_y \\ \tau_{xy} \end{Bmatrix} = [D]\{\varepsilon\} \tag{8}$$

where [D] is the stress-strain matrix and for the case of plane stress is given by

$$[D] = \frac{E}{1-\nu^2} \begin{bmatrix} 1 & \nu & 0 \\ \nu & 1 & 0 \\ 0 & 0 & (1-\nu)/2 \end{bmatrix} . \tag{9}$$

The element stiffness matrix is then:

$$[K] = \int_{-1}^{1} \int_{-1}^{1} [B]^T[D][B] \det|J| d\xi d\eta . \tag{10}$$

The integration in equation (10) is done numerically by nine-point Gaussian quadrature as explained in reference 9.

THE CRACK TIP ELEMENT

It is clear from equations (4) and (6) that we need the inverse of Jacobian matrix [J] before the strains can be computed. Hence, whenever the inverse of [J] is singular or, equivalently, the determinant of [J] is zero, the strains and stresses become singular. This is simply accomplished by placing the mid-side nodes (e.g., nodes 5 and 8 of figure 1) at quarter points

from node 1 in Cartesian coordinates.

This can be illustrated by investigating the singularity along line 1-2 (η=-1) of figure 1. Evaluating the shape functions given in figure 1 at η=-1, we have the transformation

$$x = -1/2\ \xi(1-\xi)\ x_1 + 1/2\ \xi(1+\xi)\ x_2 + (1-\xi^2)\ x_5\ . \tag{11}$$

Choosing x_1=0, x_2=L and the quarter point x_5=L/4, equation (11) becomes

$$x = 1/2\ \xi(1+\xi)L + (1-\xi^2)\ L/4 \tag{12}$$

Solving for ξ we have

$$\xi = -1 + 2\sqrt{x/L}\ . \tag{13}$$

In this case the reduced Jacobian becomes

$$\frac{\partial x}{\partial \xi} = \frac{L}{2}\ (1+\xi) = \sqrt{xL}\ . \tag{14}$$

Equation (14) clearly indicates the singularity for the inverse of the Jacobian at x=0, ξ=-1. The order of singularity can be obtained from the displacement along line 1-2 (fig. 1). From equation (2) we have

$$u(\xi,-1) = -1/2\ \xi(1-\xi)u_1 + 1/2\ \xi(1+\xi)u_2 + (1-\xi^2)u_5\ ,$$

and writing in terms of x from equation (13) we have

$$u = -1/2(-1+2\sqrt{\tfrac{x}{L}})(2-2\sqrt{\tfrac{x}{L}})u_1 + 1/2(-1+2\sqrt{\tfrac{x}{L}})(2\sqrt{\tfrac{x}{L}})u_2 + 4(\sqrt{\tfrac{x}{L}} - \tfrac{x}{L})u_5\ . \tag{15}$$

Differentiating equation (15) we obtain the strains in the x-direction:

$$\varepsilon_x = \frac{\partial u}{\partial x} = -1/2[\frac{3}{\sqrt{xL}} - \frac{4}{L}]u_1 + 1/2[\frac{-1}{\sqrt{xL}} + \frac{4}{L}]u_2 + [\frac{2}{\sqrt{xL}} - \frac{4}{L}]u_5\ , \tag{16}$$

indicating the singularity of order one-half ($\frac{1}{\sqrt{x}}$), precisely the singularity needed for crack problems. It can be seen that equation (16) also incorporates constant strain terms.

We have only investigated the singularity at node 1 along line 1-2 of figure 1. However, the singularity at node 1 along any other ray emanating from node 1 is weaker than one-half. The singularity of order one-half can simply be achieved by collapsing grid points 1, 4 and 8 and placing grid points 5 and 7 at the quarter points in Cartesian coordinates as shown in figure 2. Without loss of generality we take the Cartesian coordinates as shown. Using equations (1) and (7) it can be shown that

$$\det.|J| = 1/16\ (1+\xi)^3 \sin\alpha\ , \tag{17}$$

which vanishes for ξ=-1 for all η (i.e., along any ray from node 1). The

displacement, using polar coordinates ($x = r\cos\theta$, $y = r\sin\theta$) is given by:

$$u = 2r^{1/2}\frac{\cos^{1/2}(\theta-\alpha/2)}{\cos^{1/2}(\alpha/2)}\left[2\left(1-\frac{\cos^{1/2}(\theta-\alpha/2)}{\cos^{1/2}(\alpha/2)}r^{1/2}\right)\left\{-1/4(1-\eta)u_2 - 1/4(1+\eta)u_3 + 1/2(1-\eta)u_5 + 1/2(1+\eta)u_7\right\} - 1/4\eta(1-\eta)u_2 + 1/4\eta(1+\eta)u_3 + 1/2(1-\eta^2)u_6\right] \tag{18}$$

with

$$\eta = \frac{\tan(\theta-\alpha/2)}{\tan(\alpha/2)} . \tag{19}$$

Equation (18) indicates that the strains will have the necessary singularity of order one-half ($\frac{1}{\sqrt{r}}$) at the crack tip.

The stress intensity factors K_I and K_{II} are computed at the quarter points using the Westergaard near field displacements which, for plane stress, are given by (ref. 10).

$$\begin{aligned} u &= \frac{K_I}{G}\left(\frac{r}{2\pi}\right)^{1/2}\cos\theta/2\left[\frac{1-\nu}{1+\nu} + \sin^2\theta/2\right] + \frac{K_{II}}{G}\left(\frac{r}{2\pi}\right)^{1/2}\sin\theta/2\left[\frac{2}{1+\nu} + \cos^2\theta/2\right] \\ v &= \frac{K_I}{G}\left(\frac{r}{2\pi}\right)^{1/2}\sin\theta/2\left[\frac{2}{1+\nu} - \cos^2\theta/2\right] + \frac{K_{II}}{G}\left(\frac{r}{2\pi}\right)^{1/2}\cos\theta/2\left[-\frac{1-\nu}{1+\nu} + \sin^2\theta/2\right] \end{aligned} \tag{20}$$

Solving for K_I, K_{II} we have:

$$K_I = G\left(\frac{2\pi}{r}\right)^{1/2}\frac{u\cos\theta/2\left[-\frac{2\nu}{1+\nu} + \cos^2\theta/2\right] + v\sin\theta/2\left[\frac{2}{1+\nu} + \cos^2\theta/2\right]}{\left[\frac{2}{1+\nu} - \cos^2\theta/2\right]\left[\frac{2}{1+\nu} - \cos^2\theta/2\right]}$$

$$K_{II} = G\left(\frac{2\pi}{r}\right)^{1/2}\frac{u\sin\theta/2 - v\cos\theta/2}{\left[\frac{2}{1+\nu} - \cos^2\theta/2\right]} \tag{21}$$

THE THREE-DIMENSIONAL CASE

The three-dimensional twenty-point isoparametric quadratic 'Brick' element is formulated in much the same way, by mapping the geometry into curvilinear space (ξ,η,ζ) of a normalized cube $(-1 \leq \xi,\eta,\zeta \leq 1)$ by the quadratic shape function (ref. 9),

$$x = \sum_{i=1}^{20} N_i(\xi,\eta,\zeta)x_i \ ,$$

$$y = \sum_{i=1}^{20} N_i(\xi,\eta,\zeta)y_i \ ,$$

$$z = \sum_{i=1}^{20} N_i(\xi,\eta,\zeta)z_i \ ,$$

$$\begin{aligned} N_i = {} & 1/8(1+\xi\xi_i)(1+\eta\eta_i)(1+\zeta\zeta_i)(\xi\xi_i + \eta\eta_i + \zeta\zeta_i - 2)\ \xi_i^2\ \eta_i^2\ \zeta_i^2 \\ & + 1/4(1-\xi^2)(1+\eta\eta_i)(1+\zeta\zeta_i)(1-\xi_i^2) \\ & + 1/4(1-\eta^2)(1+\xi\xi_i)(1+\zeta\zeta_i)(1-\eta_i^2) \\ & + 1/4(1-\zeta^2)(1+\xi\xi_i)(1+\eta\eta_i)(1-\zeta_i^2) \ , \end{aligned} \tag{22}$$

where N_i is the shape function at node i (i=1 to 20) whose Cartesian and curvilinear coordinates are (x_i, y_i, z_i) and (ξ_i, η_i, ζ_i) respectively. It should be noted that the shape function given in equation (22) is obtained by superposition of those given in reference 9. The geometry of the unit cube and the numbering sequence, as suggested by reference 11, is shown in figure 3.

For the isoparametric formulation and displacements are given by

$$u = \sum_{i=1}^{20} N_i(\xi,\eta,\zeta)u_i \ ,$$

$$v = \sum_{i=1}^{20} N_i(\xi,\eta,\zeta)v_i \ , \tag{23}$$

$$w = \sum_{i=1}^{20} N_i(\xi,\eta,\zeta)w_i \ .$$

The rest of the analysis follows in a similar fashion that given for the two-dimensional case with appropriate augmentation to the three-dimensional quantities.

The singularity element is obtained by collapsing one face, 2376, and placing the midside nodes 9, 13, 11, 15 of figure 3 at quarter points. The singular element is shown in figure 4, in Cartesian coordinates. Since the elements are isoparametric they automatically satisfy inter-element compatibility and continuity in their regular or singular forms. It should be noted that the displacements are not singular. Further, it is easily shown that $\sum_i N_i=1$. Hence, by theorems given in reference 9 the elements satisfy the constant strain and rigid body modes. The above conditions are necessary for the 'patch test' mentioned in reference 2.

NASTRAN IMPLEMENTATION

The isoparametric quadratic quadrilateral and brick elements have been implemented using the NASTRAN dummy user element facility as outlined in Section 6.8.5 of reference 12. This involved coding element stiffness and stress data recovery subroutines using the analysis outlined above and relinking the affected NASTRAN Links. Additional modifications were required to some of the Output File Processor (OFP) routines. These changes are detailed below.

The quadrilateral element was implemented as a DUM1 element. Figure 5 shows the formats for the ADUM1, CDUM1 and PDUM1 cards. KDUM1, the element stiffness matrix subroutine, obtains material and grid point information from the element connection and property table (ECPT) and builds the matrices required to perform the integration in equation (10). The integration is performed numerically using compound 3-point Gaussian quadrature as explained in reference 9. This results in 9 evaluations of the integrand. Once the 16 by 16 stiffness matrix is complete, the appropriate 2 by 2 submatrices corresponding to the given pivot point are entered into the upper left of the 6 by 6 submatrices required by SMA1B, the stiffness matrix insertion subroutine. SMA1B is called 8 times for each pivot point. The time for element stiffness generation is 14 seconds per element on an IBM 360 model 44.

NASTRAN stress data recovery is accomplished in two phases. During phase I, SDUM11 calculates [D][B] from equations (5) and (9) for each grid point and passes the resultant 24 by 16 matrix to SDUM12 for final stress calculations. SDUM11 also checks for singularities in the inverse of the Jacobian (eq.(7)) and flags those grid points which have a singularity. Information passed to SDUM12 from SDUM11 includes the element id, grid point numbers, grid point singularity flag, coordinates of the eight grid points and the material constants E, G and ν. SDUM12, phase II of the stress recovery, locates the displacements associated with a given element and multiplies [D][B] times these displacements (eq. (4) and (8)) to give the stress components at each of the eight grid points. Grid point flags are checked for singular grid points and, if singularities exist, Mode I and Mode II stress intensity factors are calculated using equation (21). These stress intensity factors at the quarter points are output at the corner nodes of the collapsed side while the corresponding mid-side node stress output is set to zero. The point ids of the singular corner nodes are negated and the mid-side id is set to overflow the integer field specification, thus flagging the point with asterisks.

OFP has been modified to output the eight sets of stress components for each element. These modifications were implemented by adding heading formats to OFP1A and changing the appropriate pointers and format specifications in OFP1BD, OFP5BD and OF1PBD. Although the ADUM cards allow sufficient flexibility to implement the element stiffness subroutine, changes were required to GPTA1 which describes the connection and property characteristics of each element (see Section 2.5.2.1 in ref. 12). These changes were required to handle the expanded stress requirements. The number of words SDR2 passes from phase I to phase II was changed from 100 to 430 while the count of words SDR2 outputs for real stresses was increased from 10 to 33.

The implementation of the twenty node brick element was not as straightforward as that of the quadrilateral element. The brick was implemented as a DUM2 element. Figure 6 shows formats for the ADUM2, CDUM2 and PDUM2 cards. DIMENSION changes were required in TA1A and TA1B since NASTRAN assumes a maximum of 10 grid points per element. KDUM2 was initially implemented similarly to KDUM1. However, in this case, the integration using 3-point Gaussian quadrature requires 27 integrand evaluations with a stiffness matrix of order 60. The size of the KDUM2 subroutine necessitated a change to the overlay structure of LINK3, placing KDUM2 in its own overlay segment. Also, since NASTRAN calls the stiffness routines based upon the pivot point concept, the same brick element stiffness matrix is built twenty times in an analysis. This technique results in a 20 minute stay in SMA1 for a one element problem on an IBM 360 model 44. Changes are being made to KDUM2 to build each element stiffness matrix once and save it on auxiliary storage. When a request for an element stiffness matrix is made, KDUM2 will check auxiliary storage for a copy of the matrix. If it is not there, KDUM2 will build the matrix and add it to the file. If it is there, the matrix will be retrieved and not recalculated. Using this procedure, stiffness matrix generation should not exceed 2 minutes per element.

Stress data recovery is also non-standard for the brick element. Due to the size of the arrays used in stress recovery for the brick, phase I has a limited function of assembling arrays dependent on parameters not available to phase II. The majority of calculations for stress recovery are accomplished during phase II, saving storage but increasing stress recovery times. Quantities passed from phase I to phase II are the stress-strain matrix [D], the element id, grid point ids, grid point coordinates and the material constants E, G and ν. Phase II locates the displacements, calculates the stress components for each grid point, checks for singular Jacobians and calculates stress intensity factors as required. Stress intensity factors are displayed in a manner similar to that employed for the quadrilateral element.

OFP has been modified to output the twenty sets of stress components for each element. A DIMENSION change was also required in OFP to allow twenty grid points per element. OFP1A, OFP1BD, OFP5BD and OF1PBD were updated to produce the required heading and output formats. GPTA1 was changed to increase the number of words to 120 that SDR2 passes from phase I to phase II. The count of words SDR2 outputs for real stresses was increased to 141.

Both element implementations were checked independent of NASTRAN via dummy driver routines for SMA1 and SDR2. The coding for the element stiffness subroutines was verified by multiplying the stiffness matrix for one element times the known displacements for a uniform stress field. The resultant nodal loading was compared to that found analytically from (for the two-dimensional case)

$$\{F\}^e = \int_{-1}^{1}\int_{-1}^{1} [B]^T \{\sigma\}\, d\xi\, d\eta \qquad (24)$$

Figure 7 illustrates equivalent nodal forces for $\sigma_y = 1$ on the normalized square ($-1 \leq x,y \leq 1$). The stress recovery coding was checked by passing the known

displacements for a uniform stress field to the stress recovery subroutines and observing the constant stress results.

Implementation of the quadrilateral element was complete within a week of the completion of the analysis while the brick element implementation took 2 weeks because of the length of coding, overlay changes and NASTRAN changes to support more than 10 grid points.

NUMERICAL RESULTS

To assess the accuracy of the method, three test problems with fairly a coarse grid (68 elements and approximately 239 grid points) were run. The problems are the single edge crack, double edge crack and center crack. These three problems can be done in a single run as subcases with different single point constraints as shown in figures 8a, 8b, 8c. The solutions of above problems, by various methods, have been well documented (ref. 12). It was found that the finite element solutions were accurate to within 2-3%. Graphically, this is illustrated in figure 9 for the double edge crack by using the Westergaard near field solution (ref. 10) for σ_y.

ASTM has stringent requirements for the size of specimens for fracture toughness testing. However, in many applications of thick-walled cylinders these requirements are not easily met. The C-shaped specimen, which is easily obtained from thick-walled cylinders, was suggested (ref. 13) and is now accepted as a standard test for such cylindrical material. The stress intensity factors for such a section, shown in figure 10, were computed for different crack lengths and the finite element results, experimental results, and the collocation results of reference 13 are shown in figure 11. It is seen that remarkable agreement is obtained with just 48 elements and 171 grid points. The results have also been compared with those in reference 16 and similar correspondence was observed.

CONCLUSIONS

Quadratic isoparametric elements have been used to form a singular element for fracture mechanics analysis. These elements provide excellent results even with coarse grids as long as the singular elements strictly conform to the geometries of figures 2 and 4. The elements have been successfully implemented on NASTRAN Level 15.0 as dummy user elements.

REFERENCES

1. Henshell, R. D., and Shaw, K. G.: Crack Tip Elements are Unnecessary. Int. J. Num. Meth. Engrg, vol. 9, 1975, pp. 495-507.

2. Barsoum, Roshdy S.: On the Use of Isoparametric Finite Elements in Linear Fracture Mechanics. Int. J. Num. Meth. Engrg., vol. 10, 1976, pp. 25-76.

3. Tracey, D. M.: Finite Elements for Determination of Crack Tip Elastic Stress Intensity Factors. Eng. Fract. Mech., vol. 3, 1971, pp. 255-265.

4. Wilkinson, R. F., and Kelley, J. W.: A Failsafe Analysis Using NASTRAN's Piecewise Linear Analysis and a Nine Node Linear Element. NASTRAN: Users' Experiences, NASA TM X-3278, 1975, pp. 181-200.

5. Aberson, J. A. and Anderson, J. M.: Cracked Finite Elements Proposed for NASTRAN. NASTRAN: Users' Experiences, NASA TM X-2893, 1973.

6. Anderson, G. P., Ruggles, V. L., and Stibor, G. S.: Use of Finite Element Computer Programs in Fracture Mechanics. Int. J. Fract. Mech., vol. 7, March 1971, pp. 63-76.

7. Chan, S. K., Tuba, I. S., and Wilson, W. K.: On the Finite Element Method in Linear Fracture Mechanics. Eng. Fract. Mech., vol. 2, no. 1, 1970, pp. 1-17.

8. McDonough, J. R.,: A Survey of NASTRAN Improvements Since Level 15.5. NASTRAN: Users' Experiences, NASA TM X-3278, 1975, pp. 11-22.

9. Zienkiewicz, O. O.: The Finite Element Method in Engineering Science. McGraw Hill, London, 1971.

10. Fracture Toughness Testing and Its Applications. ASTM, STP 381, pp. 32-33.

11. Wahlstron, Stig: Solid Element Requirements for NASTRAN. NASTRAN Users' Experiences, NASA TM X-2378, 1971, pp. 797-811.

12. The NASTRAN Programmer's Manual. NASA SP-223(01), Sept. 1972.

13. Tada, H., Paris, C. P. and Irwin, G. R.: The Stress Analysis of Cracks Handbook. Del Research Corporation, 1973, pp. 2.1-2.11.

14. Kendall, D. P. and Hussain, M. A.: A New Fracture-Toughness Test Method for Thick-Walled Cylinder Material. Experimental Mechanics, April 1972, pp. 184-189.

15. Hussain, M. A., Lorensen, W. E., Kendall, D. P., and Pu, S. L.: A Modified Collocation Method for C-Shaped Specimens. Watervliet Arsenal Tech. Report, R-WVT-X-6-73, 1973.

16. Gross, B. and Srawley, J. E.: Analysis of Radially Cracked Ring Segments Subject to Forces and Couples. NASA TM X-71842, 1976.

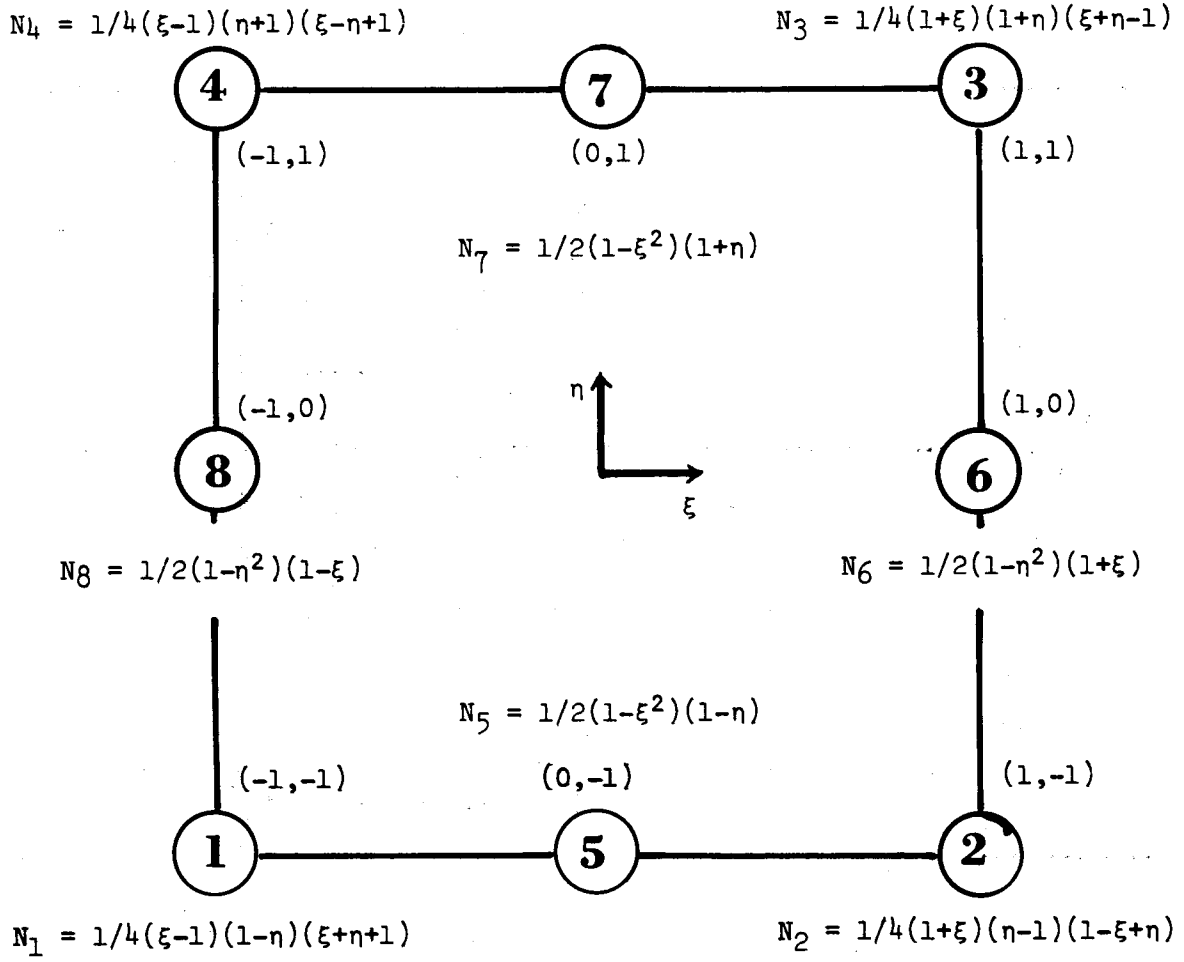

Figure 1. - Shape Functions and Numbering Sequence for Quadrilateral Element.

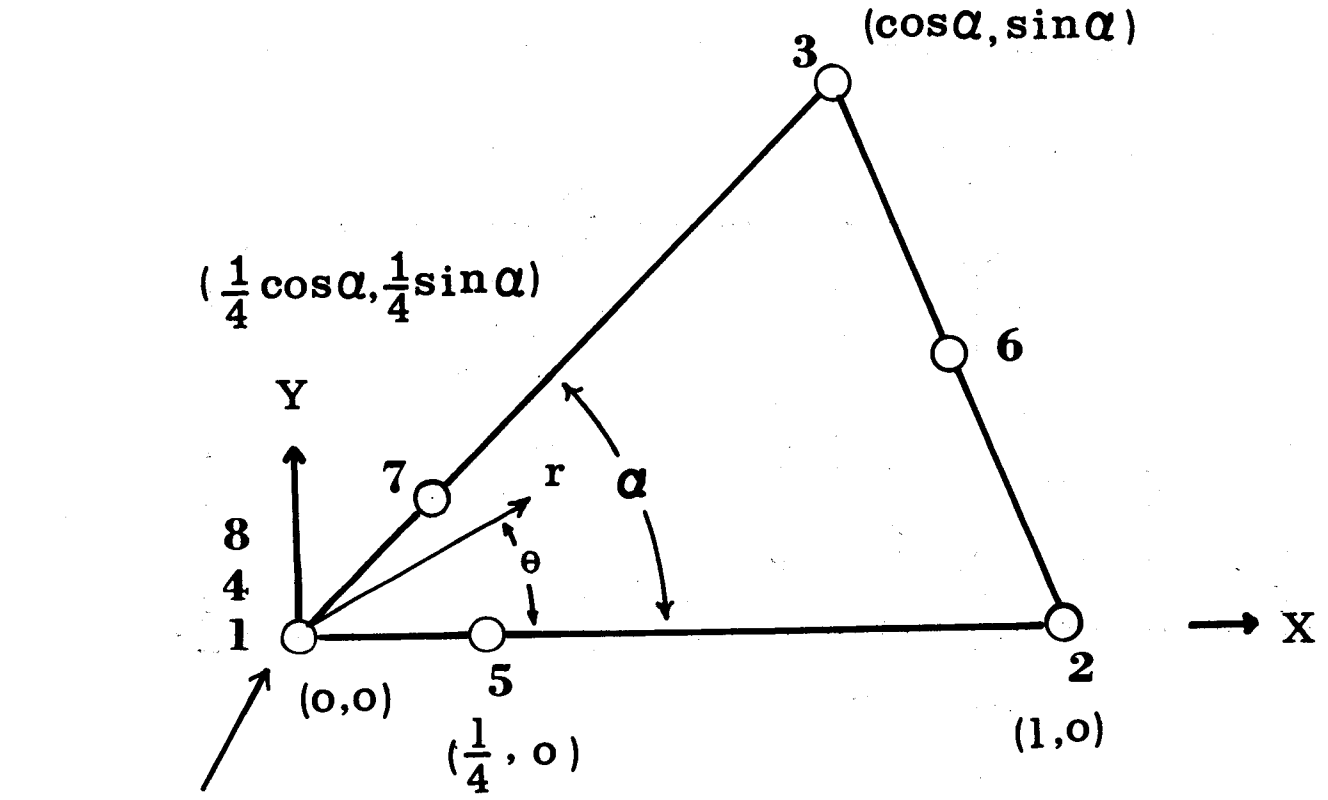

Figure 2. - Singularity Element Obtained by Collapsing 1, 4 and 8 and placing 5 and 7 at Quarter Points.

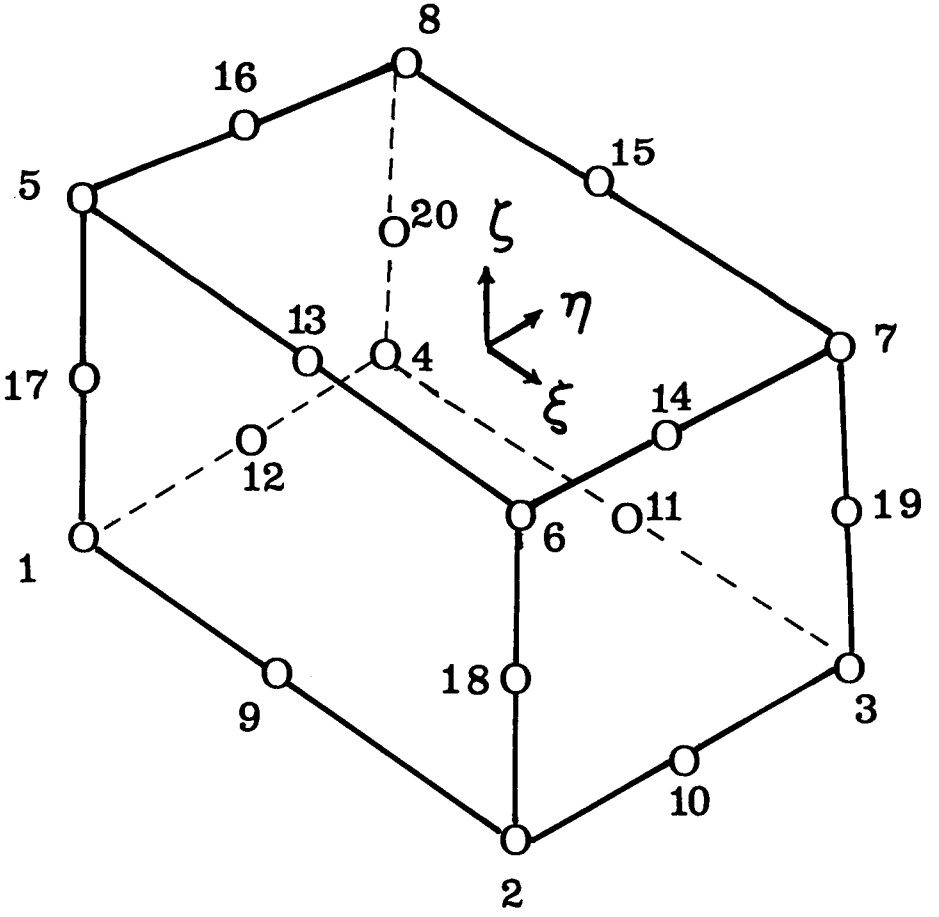

Figure 3. - Numbering Sequence of Isoparametric Quadratic 'Brick' Element.

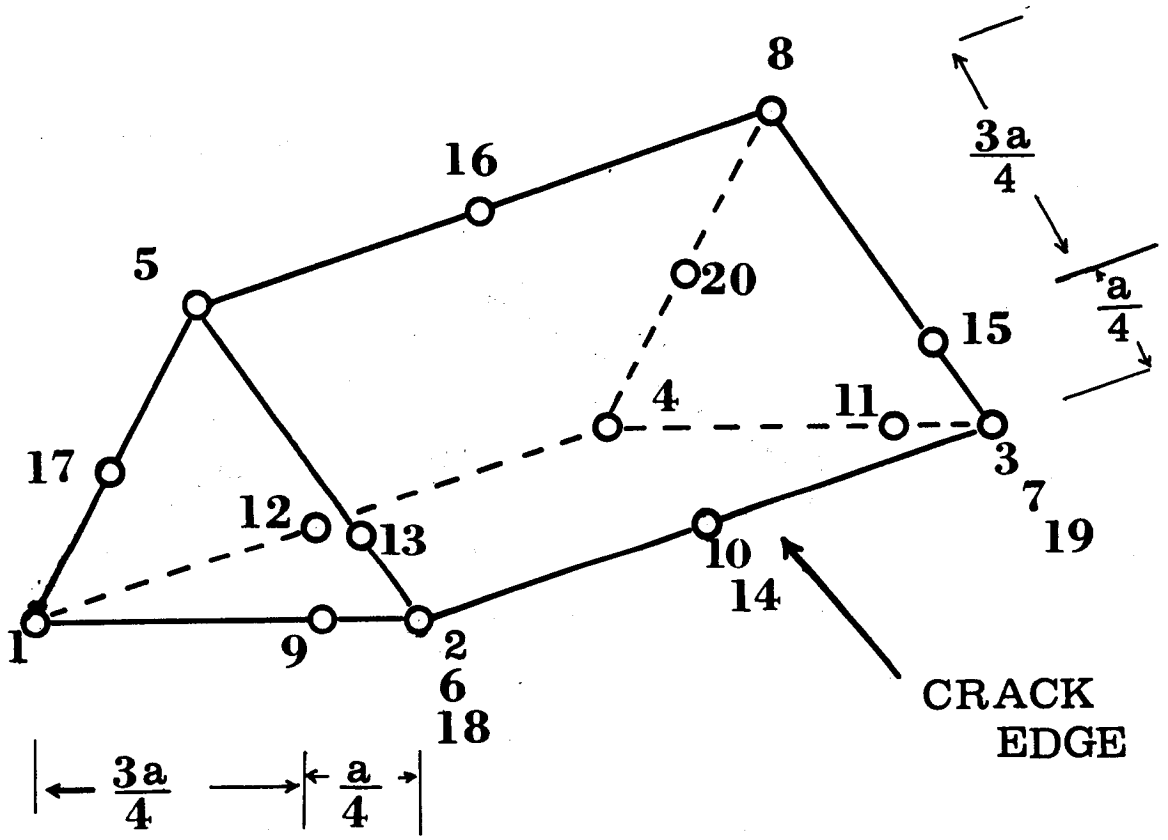

Figure 4. - Singularity Element Obtained by Collapsing the Face 2376 and Placing the Nodes 9, 13, 11 and 15 at Quarter Points.

ADUMi	NG	NC	NP	ND					
ADUM1	8	0	1	3					

CDUMi	EID	PID	G1	G2	G3	G4	G5	G6	abc
CDUM1	1	10	1	2	3	4	5	6	abc

+bc	G7	G8							
+bc	7	8							

PDUMi	PID	MID							
PDUM1	10	20							

Figure 5. Bulk Data Cards for Quadrilateral Element.

ADUMi	NG	NC	NP	ND					
ADUM2	20	0	1	3					

CDUMi	EID	PID	G1	G2	G3	G4	G5	G6	abc
CDUM2	1	10	1	2	3	4	5	6	abc

+bc	G7	G8	G9	G10	G11	G12	G13	G14	def
+bc	7	8	9	10	11	12	13	14	def

+ef	G15	G16	G17	G18	G19	G20			
+ef	15	16	17	18	19	20			

PDUMi	PID	MID							
PDUM2	10	20							

Figure 6. Bulk Data Cards for Brick Element.

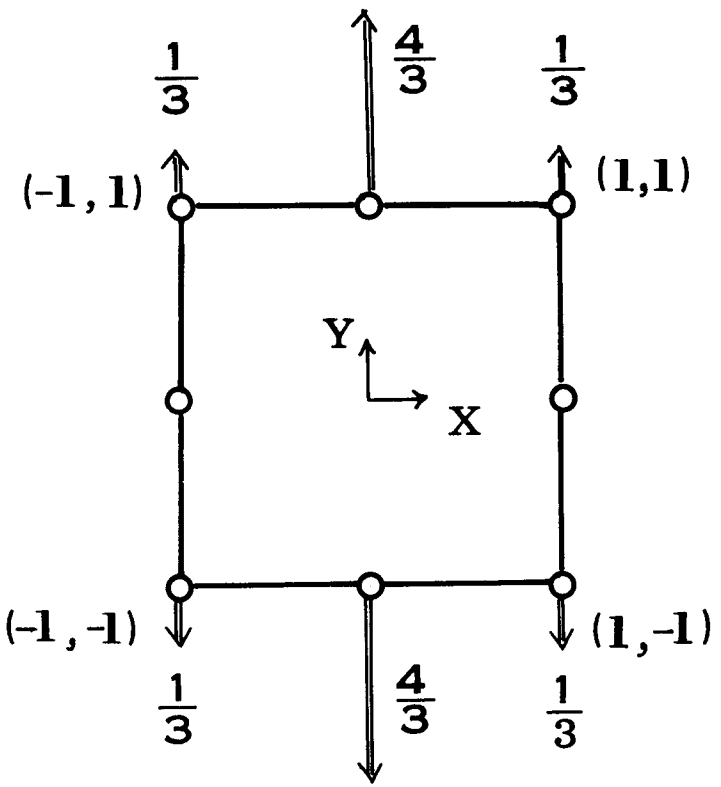

Figure 7. - Equivalent Nodal Forces Required for σy=1.

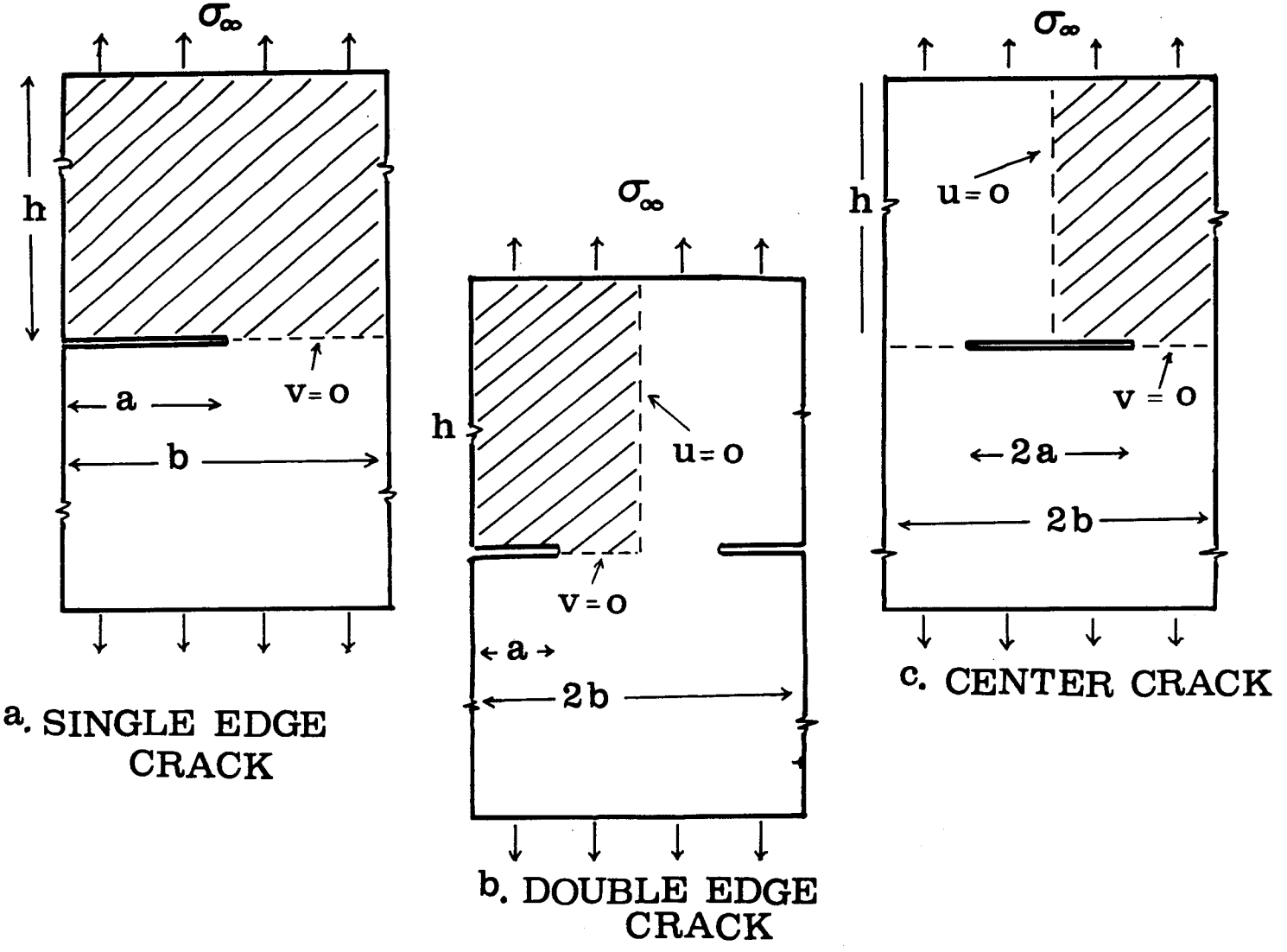

Figure 8. - Test Problem: Shaded Area Analysed by Finite Elements. ($\frac{a}{b}=\frac{1}{2}, \frac{h}{b}=4$)

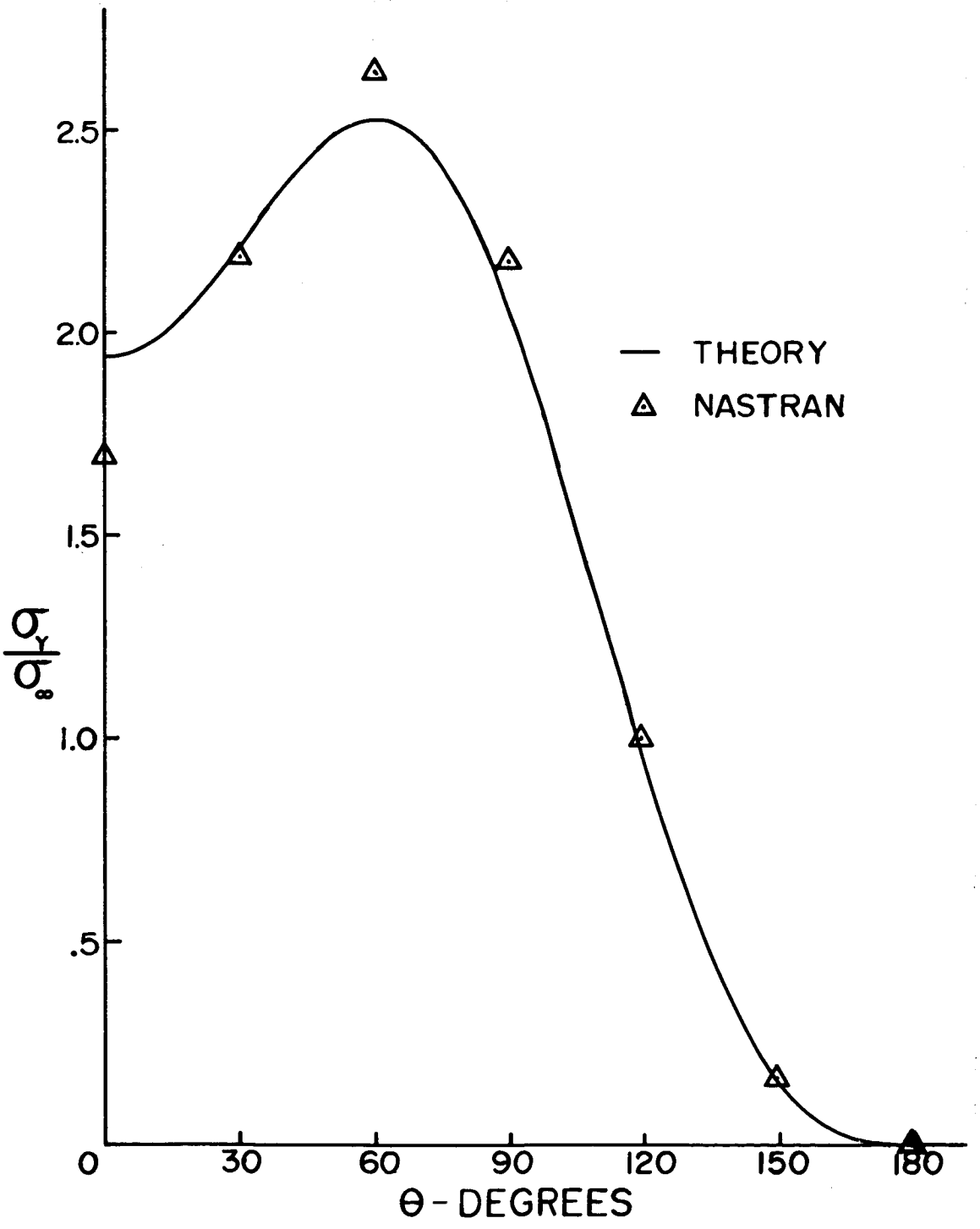

Figure 9. - Comparison of NASTRAN Results With the Theoretical Solution for Double-Edge Crack.

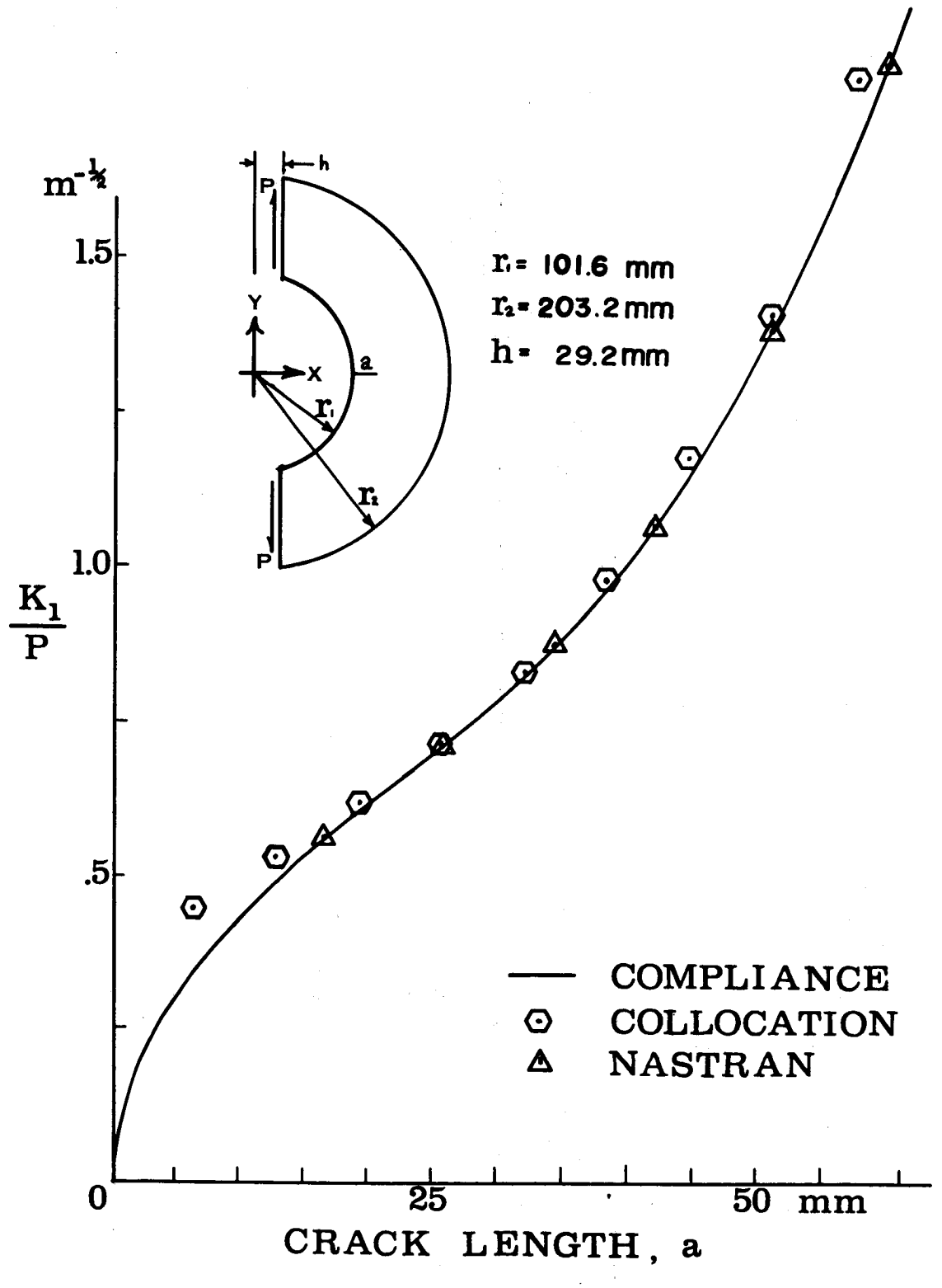

Figure 10. - Comparison of NASTRAN Results With Those Obtained Experimentally and by Collocation.